

# Early Time Interaction of Lithium Ions With the Solar Wind in the AMPTE Mission

A. T. Y. LUI

*The Johns Hopkins University Applied Physics Laboratory, Laurel, Maryland*

C. C. GOODRICH

*Department of Physics and Astronomy, University of Maryland, College Park*

A. MANKOFSKY

*Science Applications International Corporation, McLean, Virginia*

K. PAPADOPOULOS

*Department of Physics and Astronomy, University of Maryland, College Park*

The early time interaction of an artificially injected lithium cloud with the solar wind is simulated with a one-dimensional hybrid code. Simulation results indicate that the lithium cloud presents an obstacle to the solar wind flow, forming a shock-like interaction region. Several notable features are found: (1) The magnetic field is enhanced up to a factor of about 6, followed by a magnetic cavity downstream. (2) Solar wind ions are slowed down inside the lithium cloud, with substantial upstream reflection. (3) Most of the lithium ions gradually pick up the velocity of the solar wind and move downstream. (4) Intense and short-wavelength electric fields exist ahead of the interaction region. (5) Strong electron heating occurs within the lithium cloud. (6) The convection electric field in the solar wind is modulated in the interaction region. The simulation results are in remarkable agreement with in situ spacecraft measurements made during lithium releases in the solar wind by the AMPTE (Active Magnetospheric Particle Tracer Explorers) Program.

## INTRODUCTION

In September 1984 the Active Magnetospheric Particle Tracer Explorers (AMPTE) mission successfully released two lithium clouds in the solar wind [Krimigis *et al.*, 1982; G. Haerendel *et al.*, unpublished manuscript, 1985]. A primary task in the active aspect of the mission is to investigate the interaction of the solar wind with the injected clouds. Prior to these releases, several theoretical studies predicting the various aspects of the injection had been conducted [Winske *et al.*, 1984; Brinca, 1984; Decker *et al.*, 1983, 1984; Olson and Pfizter, 1984]. Some of these studies treat the lithium ions as test particles and assess their energization and subsequent paths through the solar wind-magnetosphere system downstream of the released point [Haerendel and Papamastorakis, 1983; Decker *et al.*, 1983, 1984; Brinca, 1984; Olson and Pfizter, 1984]. Other studies [Hausler *et al.*, 1983; Papadopoulos, 1983; Winske *et al.*, 1984] concentrate on the collective behavior of the artificial lithium ions. It has been suggested [Papadopoulos, 1983] that collective plasma phenomena are crucial in understanding the early time interaction of the lithium ions with the solar wind.

The purpose of this paper is to present results from numerical simulations with a one-dimensional hybrid code on the collective behavior of the lithium cloud during its early time development, i.e. less than 30 s following the release of lithium in the solar wind. Emphasis is given to the modification of the natural environment by the artificially injected ions that essen-

tially form an obstacle to the flow of the solar wind plasma. The simulation results are in good quantitative agreement with the spacecraft observations in the vicinity of the release site.

## DESCRIPTION OF MODEL

The present simulation is performed with a hybrid code in which the solar wind and lithium ions are treated kinetically as particles, while the electrons are represented by a massless fluid. All three velocity components are retained, but the spatial variation is allowed in one dimension only (the  $x$  direction). The ion motion is calculated by the particle-in-cell (PIC) technique from the equation of motion

$$m_i \frac{dv_i}{dt} = e (\mathbf{E} + \mathbf{v}_i \times \mathbf{B}) + \mathbf{P} \quad (1)$$

where  $\mathbf{P}$  is the mean frictional force imposed by the electrons and is related to the current  $\mathbf{J}$  and the "anomalous" resistivity  $\eta$  (treated as a constant) by  $\mathbf{P} = -\eta e \mathbf{J}$ . The electron fluid motion is governed by the momentum equation

$$n_e m_e \frac{dv_e}{dt} = -en_e (\mathbf{E} + \mathbf{v}_e \times \mathbf{B}) - \nabla p_e - n_e \mathbf{P} = 0 \quad (2)$$

where  $p_e$  and  $\mathbf{v}_e$  represent the electron pressure and bulk velocity, respectively. The final equality in the above equation results from neglecting the electron mass. We determine  $p_e$  from the isotropic energy equation including ohmic heating due to the anomalous resistivity  $\eta$ . Quasi-neutrality is assumed so that the electron and total ion densities are equal ( $n_e = \Sigma n_i$ ). Quasi-neutrality further requires that  $\nabla \cdot \mathbf{J} = 0$ , which in one-

Copyright 1986 by the American Geophysical Union.

Paper number 5A8520.  
0148-0227/86/005A-8520\$05.00

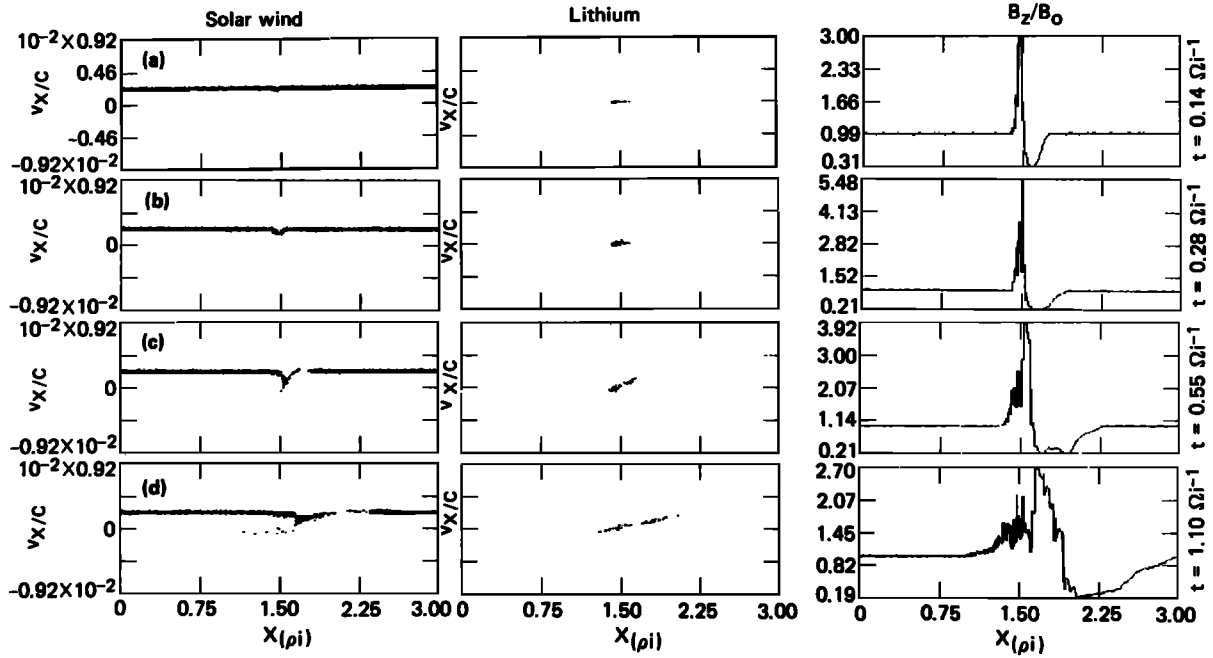


Fig. 1. Phase space plots of solar wind ions and lithium ions and profile of the magnetic field (dawn-to-dusk component, normalized to its initial value) at four different time steps. At the interaction region, the solar wind ions slow down with some ions reflected upstream ( $v_x < 0$ ), while the lithium ions are seen to spread spatially and are accelerated downstream. The magnetic field is compressed at the front portion of the lithium cloud followed downstream by a magnetic cavity. The largest field compression is about 5.5. Complex magnetic field structures develop when reflected solar wind ions begin to gyrate back into the interaction region.

dimension determines  $v_{ex} = \Sigma_i n_i V_{ix} / \Sigma_i n_i$ . Assuming that  $\mathbf{B}$  is in the  $z$  direction, Maxwell's equations and the  $y$  component of the electron momentum equation determine the vector potential  $A_y$ ,

$$\frac{\eta}{\mu} \frac{\partial^2 A_y}{\partial x^2} = v_e \frac{\partial A_y}{\partial x} \quad (3)$$

The calculation scheme starts from given  $\mathbf{E}$ ,  $\mathbf{B}$ , and  $\mathbf{J}$  to solve for the ion motions with equation (1), which in turn allows  $A_y$  in equation (3) to be determined by the algorithm given by *Sgro and Nielson* [1976]. The new values of  $\mathbf{E}$ ,  $\mathbf{B}$ , and  $\mathbf{J}$  at the next time step are then derived. The details of the numerical scheme can be found in the work by *Leroy et al.* [1982]. The advantages and limitations of the hybrid code for simulation of space plasma physics are discussed by *Goodrich* [1985].

#### INITIAL CONDITIONS

In this simulation, the solar wind plasma is injected from the left into the simulation box as a convecting Maxwellian population with a bulk flow of  $V$  in the  $x$  direction. The magnetic field is assumed to be transverse to the solar wind flow, in the  $z$  direction. The ion density and magnetic field in the solar wind are taken to be  $10 \text{ cm}^{-3}$  and  $10 \text{ nT}$ , respectively. The Alfvén Mach number ( $M_A = v_i \sqrt{\mu_0 n_i m_i / B}$ ) of the solar wind flow is 10. Solar wind electron and ion betas are set to 1. The resistivity  $\eta$  used is  $1.2 \times 10^{-4} \omega_{pi}^{-1}$ , where  $\omega_{pi}^{-1}$  is the ion plasma frequency in the solar wind. This value of resistivity corresponds to a collision frequency of about  $4 \times 10^{-4} \omega_{pe}$ , where  $\omega_{pe}$  is the electron plasma frequency in the solar wind. The total length of the box is about three times the solar wind ion gyroradius. More than 10,000 simulation particles in 600 cells are used.

As mentioned in the introduction, our study emphasizes the collisionless plasma coupling aspects between the solar wind and the ionized part of the lithium at early times. For this reason, we neglect the neutral lithium and assume the ionized lithium density to be constant over the time scale of interest (i.e., a few seconds). The lithium ions and their associated electrons are initialized cold (ion and electron beta smaller than  $10^{-3}$ ); the lithium ions are given an isotropic Maxwellian velocity distribution at rest in the simulation frame. The average ionized lithium density is taken as  $50 \text{ cm}^{-3}$  and is distributed over 32 km, with a Gaussian density profile. This ion cloud corresponds to about 0.03% ionization of the neutrals, assuming a yield of  $2 \times 10^{25}$  lithium atoms in the release. The spatial profile of the number density is consistent with that expected on the basis of photoionization of a neutral cloud [*Decker et al.*, 1984], and the cloud size is compatible with in situ observation (*G. Haerendel et al.*, unpublished manuscript, 1985).

#### SIMULATION RESULTS

The time development of the phase space density ( $v_x, x$ ) of the solar wind and lithium ions, as well as the magnetic field profile, is shown in Figure 1. The time is scaled in  $\Omega_i^{-1}$ , where  $\Omega_i$  is the ion gyrofrequency in the solar wind. The top row of panels, which correspond to a time  $t = 0.14 \Omega_i^{-1}$  after the release, indicate very little modification on the solar wind and lithium distribution. However, the magnetic field is amplified to about three times its initial value. Behind the field compression region, there is a magnetic field cavity. At time  $t = 0.28 \Omega_i^{-1}$ , the deceleration of the solar wind ions within the cloud becomes apparent. The decrease in the solar wind flow is most prominent toward the upstream half of the lithium cloud. There is a slight but noticeable increase in the velocity of the lithium

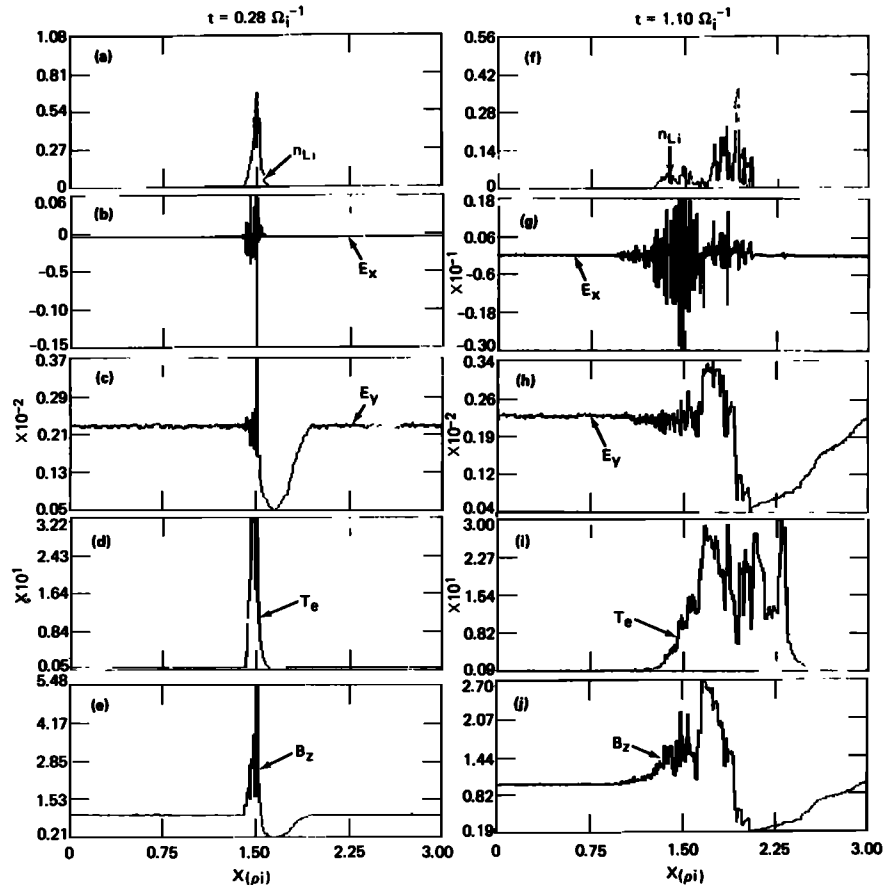


Fig. 2. Plots of lithium number density (normalized to its initial maximum value), electric field components (normalized to the initial magnetic field), electron temperature (normalized to its initial temperature), and magnetic field (dawn-to-dusk component) at two different times: (a-e) at  $t = 0.28 \Omega_i^{-1}$  and (f-j) at  $t = 1.10 \Omega_i^{-1}$ . The  $x$  direction is pointing antisunward and the  $y$  direction is toward north. The compressed magnetic field occurs within the lithium cloud and the magnetic cavity occurs downstream. At the later time, the  $x$  component of the electric field is most intense upstream of the magnetic field compression region.

ion, mainly in the downstream portion of the cloud at this time. The magnetic field compression has grown. Over a major extent of the lithium cloud, especially in the upstream half, the magnetic field is enhanced to a maximum factor of about 5.5. The magnetic cavity is seen to extend further downstream. At later times (the third and fourth rows), the lithium cloud is seen to spread further spatially, with the main population shifted substantially downstream. This is a result of the partial transfer of the solar wind momentum to the lithium ions evident in the phase space plots. The primary force that moves the lithium ions is electric, since these ions have negligible  $V_y$  component. These changes are accompanied by reflection of some solar wind ions that flow upstream of the main solar wind population. The magnetic field at these later times has a rather complex structure with the magnetic cavity stretching further downstream.

The location of the cloud in relation to the dynamic structures in the magnetic field, electric fields ( $E_x$ ,  $E_y$ ), and electron temperature ( $T_e$ ) is shown in Figure 2 for two time steps. The electric field can be converted to millivolts per meter by multiplying the plotted values by 3000. Note that the bulk of the lithium is located just upstream of the magnetic cavity at both times. Strong, dynamic electric fields in the direction of the flow of the solar wind are built up, especially in the upstream half of the lithium cloud. It is found that the fluctua-

tions of the electric field are insensitive to variations of resistivity and cell size in the simulation and are therefore unlikely to be a numerical artifact. The convection electric field  $E_y$  is also enhanced just near the cloud center, but is much reduced from its upstream value in the magnetic cavity. Electron heating is found in regions of high magnetic field.

#### PHYSICAL INTERPRETATION OF THE RESULTS

The development of the magnetic field compression and the associated laminar electric fields can be understood from the following physical considerations. Since the electron gyroradius is very small, a fluid description in which the magnetic field and the solar wind electrons move together is adequate. At the early time (i.e.,  $\Omega_i t < 1$ ), the solar wind ions are unaffected by the magnetic field and penetrate freely inside the lithium cloud, being neutralized by the electrons inside the lithium cloud. Meanwhile the solar wind electrons and their associated magnetic field pile up in a shell with the magnetic field compressed near the interface, as shown schematically in Figure 3. The solar wind electrons are heated during this compression by a combination of adiabatic and ohmic heating. The latter results from anomalous dissipation of the cross-field current responsible for the field compression and is the dominant factor. This electron heating is clearly a significant effect in this interaction although hybrid simulations in general tend to overestimate its absolute

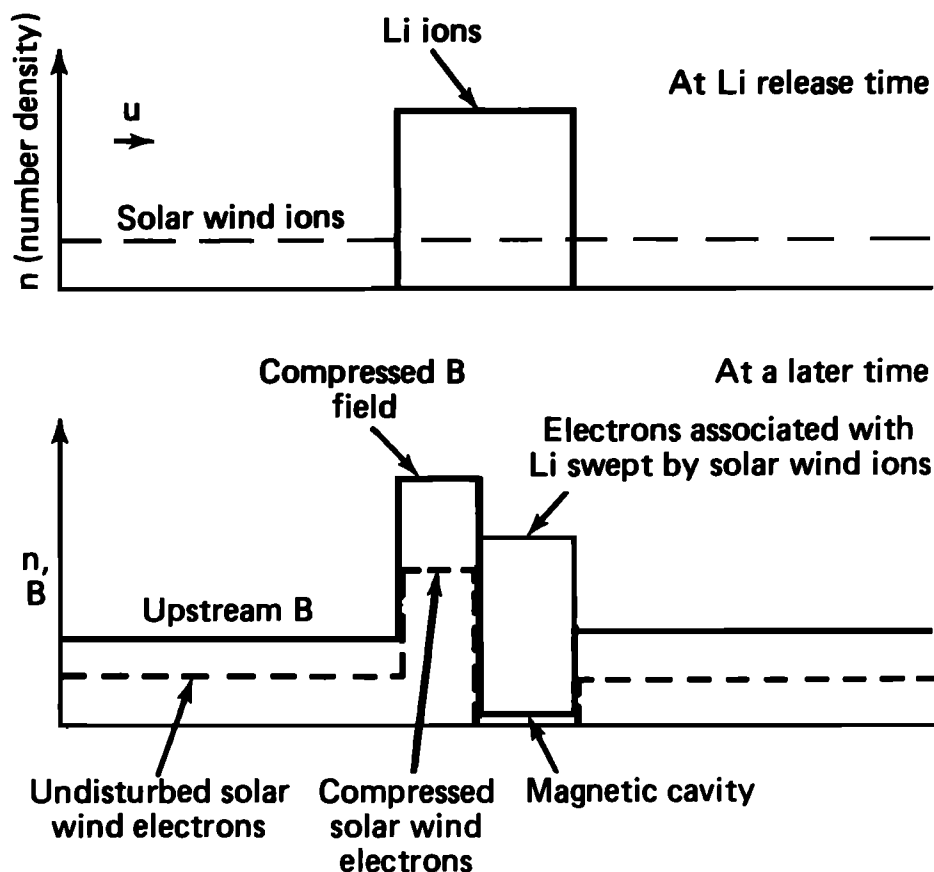


Fig. 3. A schematic diagram to illustrate the physical process by which the magnetic field compression and cavity are formed.

magnitude. An analytic solution to this problem including the role of the electron inertia, resistivity, and whistler structure has been discussed briefly by Papadopoulos [1983, 1985] and will be presented in detail in a later paper.

The piling-up process must continue until laminar electric fields or instabilities develop that invalidate the assumption of undisturbed solar wind ion motion. In our simulations (Figures 1b, 2b), the laminar potential associated with the compressed shell becomes large enough to stop or reflect the incoming solar wind ions, thereby preventing any further compression. The laminar forces also accelerate the lithium ions to a significant fraction of the solar wind velocity at later times. The reflected ions gyrate and reenter the downstream region causing the development of magnetic field structure. The situation is reminiscent of the quasi-perpendicular bow shock [Leroy *et al.*, 1981, 1982; Forstlund *et al.*, 1984], with roughly 10–20% of the particles being reflected. The complex local ion counterstreaming among the reflected and incoming solar wind ions as well as the relatively stationary lithium ions is the probable cause of the electrostatic noise seen in Figure 2g at later times. The interaction seen is similar to the classic collisionless piston formation in colliding high Mach number plasma streams [Clark *et al.*, 1973].

#### COMPARISON WITH OBSERVATIONS

The in situ spacecraft observations of the magnetic and electric fields are shown in Figure 4 [Hausler *et al.*, this issue]. This is taken during the second solar wind release on September 20, 1984. Before the release, the ambient magnetic field is about

8.6 nT and is fairly steady. About 2 s after the release, the magnetic field decreases to practically zero for about 7 s. Sharp recovery of the magnetic field component perpendicular to the solar wind flow is found to be amplified by a factor of 6. The magnetic field remained compressed for about 11 s, gradually declining to the prerelease value. The electric field from the plasma wave instrument is found to be enhanced upstream of the compressed magnetic field region, spatially distinct from the sharp magnetic field gradient where intense diamagnetic current flows.

This time profile of magnetic field can be compared with the simulation results in the following fashion. The initial drop in the magnetic field corresponds to the entry of the spacecraft into the magnetic cavity after about 2 s of the release. As time progresses, the magnetic field structure is gradually carried downstream by the solar wind, allowing the spacecraft to sweep through the magnetic field structure. Note that the peak in the electric wave field measurements being delayed with respect to the peak in the magnetic field compression is consistent with the simulation result that intense electric field fluctuations exist ahead of the magnetic shell and in the reflection region (i.e., the magnetic foot). Although ion counterstreaming is suggested here as the cause of the observed fluctuations in the electric field, there are also other likely candidates such as the electron-ion instabilities studied for the case of quasi-perpendicular shock waves by Wu *et al.* [1984].

A number of other significant features of the simulation results may provide further comparison with in situ measurements.

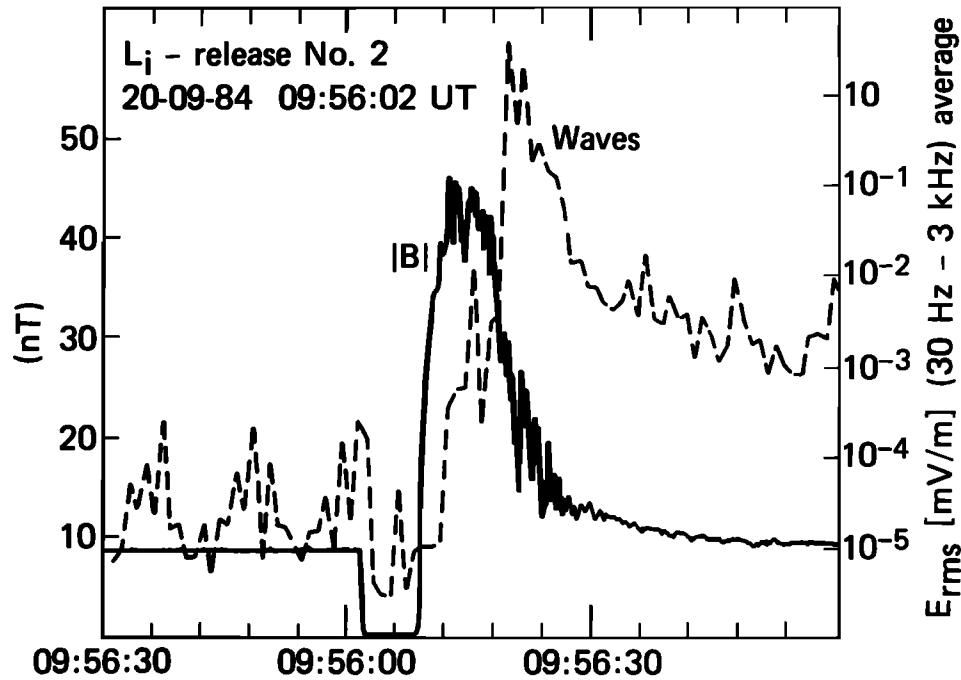


Fig. 4. Observations of the solar wind magnetic field and plasma wave intensity after a lithium release on September 20, 1984 [Hausler et al., this issue].

1. Lithium ions gradually pick up velocities from the solar wind and move downstream.
2. Electrons are heated in association with the amplification of the magnetic field compression.
3. Some solar wind ions are reflected in front of the lithium cloud.
4. Multiple magnetic field structures develop when the reflected solar wind ions gyrate back into the interaction region.
5. The convection electric field in the solar wind is modulated by the interaction to become very nonuniform.

There is one notable feature in which the simulation results differ from the observations. The magnetic field compression in our simulation is reduced within a time scale of the order of 1 s rather than  $\sim 10$  s as observed in the AMPTE program. There are several possible explanations for this disparity. First, the lithium cloud is initially seeded in the simulation experiment and no additional lithium ions are added later. In the actual situation, the un-ionized neutral lithium expands from the release point and becomes ionized gradually. This leads to the appearance of new shells of lithium ions at increasing distance from the release site as time progresses. The additional lithium ions upstream of the initial lithium cloud are likely to enhance and sustain the magnetic field compression. Secondly, the decrease in  $B$  in the simulation results is largely due to the upstream motion of the reflected solar wind ions. In the one-dimensional geometry of the hybrid code, these ions are directly upstream of the lithium cloud and eventually reenter it. In the actual AMPTE release, the lithium cloud had a finite extent, so that the reflected ions would move across, and possibly beyond, the cloud. Certainly, for a portion of the cloud surface, solar wind ions would be slowed and reflected, but no ion would be able to return. This would result in a significantly different evolution in  $B$  from that seen in the simulation at later times. In addition, the finite size of the actual lithium cloud that allows solar wind ions to exert a lateral pressure on the

interaction region would lead to a reduction in the downstream extent of the magnetic cavity predicted by this one-dimensional hybrid simulation. Finally, the assumption of no additional lithium ionization within the cloud is equivalent to assuming  $\tau_{\text{ion}} \gg \tau_0$ , where  $\tau_{\text{ion}}$  is the ionization time and  $\tau_0$  is the time scale of the simulated phenomena. While this is well satisfied if  $\tau_{\text{ion}}$  is due to photoionization, it is questionable when electron heating is observed in the compressed shell in the simulations as well as by the AMPTE instruments near the release location. Notice that the electron temperature is of the order of 50–100 eV. Since their density is equal to the lithium density, the lithium ionization rate will be given by

$$\frac{dn_{\text{Li}}}{dt} = n_{\text{Li}} N \langle \sigma V_e \rangle \approx 5 \times 10^{-8} \times n_{\text{Li}} N$$

where  $N$  is the neutral lithium density in units of  $\text{cm}^{-3}$ . The ionization time scale is given by

$$\tau_{\text{ion}} = \frac{10^8}{5N}$$

For a release yield of  $\sim 10^{25}$  lithium atoms expanding at a speed of 3.7 km/s, we have

$$N \approx \frac{10^{25}}{(3.7 \times 10^5)^3 t^3} = \frac{2 \times 10^8}{t^3}$$

$$\frac{\tau_{\text{ion}}}{t} = \frac{t^2}{10}$$

Thus the ionization due to the hot electrons cannot be ignored on the time scale of the compression and of our simulations. The neglect of this effect in our simulations may also be respon-

sible for rapid reduction of the field compression with a time scale of the order of 1 s rather than the 6–10 s as observed in the AMPTE releases. Results with a new version of the code that includes expanding shells of lithium ions, ionization due to both hot electrons and photoionization, and two-dimensional effects currently under progress will be presented in the future.

#### CONCLUSIONS

The lithium releases in the AMPTE program provide us with an opportunity to test our theoretical understanding and predictions on the interaction of a cold plasma injected in a hot plasma flowing at super-Alfvénic speed. The plasma physics aspects of this interaction are emphasized in this study by performing plasma simulation with a hybrid code. Although the code is limited to one dimension, it is found that several notable features from the simulation results agree remarkably well with existing in situ observations. This favorable comparison suggests that the simulation captures the essential physics involved in understanding the early time behavior of this active experiment performed by the AMPTE team. The results also demonstrate that collective behavior of the two plasmas is of crucial importance in the early time development of the lithium cloud in the solar wind.

*Acknowledgments.* We are grateful to S. M. Krimigis and G. Haerendel for discussions on solar wind releases from the AMPTE program. This work is supported in part by the Department of the Navy, Naval Sea Systems Command, under contract N00024-83-C-8301 to The Johns Hopkins University Applied Physics Laboratory. It is also supported in part by the Solar Terrestrial Theory Program, NASA grant NAGW-81, to the University of Maryland, and National Science Foundation travel grant INT 83-04379.

The Editor thanks E. Mobius and D. Winske for their assistance in evaluating this paper.

#### REFERENCES

- Brinca, A. L., Ion propagation in the magnetosheath, *J. Geophys. Res.*, **89**, 7339, 1984.
- Clark, R. W., J. Denavit, and K. Papadopoulos, Laminar interactions in high Mach number plasma flows, *Phys. Fluids*, **16**, 1097, 1973.
- Decker, R. B., A. T. Y. Lui, and S. M. Krimigis, Modeling of interaction of artificially released lithium with the earth's bow shock, *Geophys. Res. Lett.*, **10**, 525, 1983.
- Decker, R. B., L. Vlahos, and A. T. Y. Lui, Predictions of lithium interactions with earth's bow shock in the presence of wave activity, *J. Geophys. Res.*, **89**, 7331, 1984.
- Forsslund, D. W., K. Quest, J. U. Brackbill, and K. Lee, Collisionless dissipation in quasi-perpendicular shocks, *J. Geophys. Res.*, **89**, 2142, 1984.
- Goodrich, C. C., Numerical simulations of quasi-perpendicular collisionless shocks, in *Collisionless Shocks in the Heliosphere: Reviews of Current Research, Geophys. Monogr. Ser.*, vol. 35, edited by B. T. Tsurutani and R. G. Stone, pp. 153–168, AGU, Washington, D.C., 1985.
- Goodrich, C. C., K. Papadopoulos, and J. D. Huba, Early time coupling studies using a 1-D hybrid code, *NRL Memo.*, in press, 1985.
- Haerendel, G., and I. Papamastorakis, Refraction and reflection of seeded ions at the bow shock, *Rep. ASP03*, Inst. für extraterr. Phys., Max-Planck-Inst. für Phys. und Astrophys., Garching, Federal Republic of Germany, 1983.
- Hausler, B., R. Treumann, G. Haerendel, and E. Mobius, Wave effects expected during the AMPTE-Li-cloud release in the solar wind, *Eos Trans. AGU*, **64**, 794, 1983.
- Hausler, B., et al., Plasma waves observed by the IRM and UKS spacecraft during the AMPTE solar wind lithium releases: Overview, *J. Geophys. Res.*, this issue.
- Krimigis, S. M., G. Haerendel, R. W. McEntire, G. Paschmann, and D. A. Bryant, The Active Magnetospheric Particle Tracer Explorers Program, *Eos Trans. AGU*, **63**, 843, 1982.
- Leroy, M. M., C. C. Goodrich, D. Winske, C. S. Wu, and K. Papadopoulos, Simulations of a perpendicular bow shock, *Geophys. Res. Lett.*, **8**, 1269, 1981.
- Leroy, M. M., D. Winske, C. C. Goodrich, C. S. Wu, and K. Papadopoulos, The structure of perpendicular bow shocks, *J. Geophys. Res.*, **87**, 5081, 1982.
- Olson, W. P., and K. A. Pfizter, The entry of AMPTE lithium ions into a magnetically closed magnetosphere, *J. Geophys. Res.*, **89**, 7347, 1984.
- Papadopoulos, K., Early ionization and coupling of the AMPTE releases to the solar wind plasma, *Eos Trans. AGU*, **64**, 794, 1983.
- Papadopoulos, K., Microinstabilities and anomalous transport, in *Collisionless Shocks in the Heliosphere: A Tutorial Volume, Geophys. Monogr. Ser.*, vol. 34, edited by R. G. Stone and B. T. Tsurutani, pp. 59–90, AGU, Washington, D.C., 1985.
- Sgro, A. G., and C. W. Nielson, Hybrid model studies of ion dynamics and magnetic field diffusion during pinch implosions, *Phys. Fluids*, **19**, 126, 1976.
- Winske, D., C. S. Wu, Y. Y. Li, and G. C. Zhou, Collective capture of released lithium ions in the solar wind, *J. Geophys. Res.*, **89**, 7327, 1984.
- Wu, C. S., D. Winske, Y. M. Zhou, S. T. Tsai, P. Rodriguez, M. Tanaka, K. Papadopoulos, K. Akinoto, C. S. Lin, M. M. Leroy, and C. C. Goodrich, Microinstabilities associated with a high Mach number, perpendicular bow shock, *Space Sci. Rev.*, **37**, 63, 1984.
- C. C. Goodrich, Department of Physics and Astronomy, University of Maryland, College Park, MD 20742.
- A. T. Y. Lui, Applied Physics Laboratory, The Johns Hopkins University, Laurel, MD 20707.
- A. Mankofsky, Science Applications International Corporation, 1710 Goodridge Drive, P. O. Box 1303, McLean, VA 22102.
- K. Papadopoulos, Department of Physics and Astronomy, University of Maryland, College Park, MD 20742.

(Received February 7, 1985;  
revised April 11, 1985;  
accepted April 11, 1985.)